

# Analytical Insights Into Outage Probability and Ergodic Capacity of Fluid Antenna Systems

Hui Zhao and Dirk Slock

**Abstract**—This letter analyzes the delivery performance of a point-to-point (P2P) fluid antenna system (FAS), where the receiver is equipped with a one-dimensional  $N$ -port fluid antenna. For the first time, we *rigorously* reveal the diversity order of the P2P FAS through mathematical proof. Motivated by this analysis, we propose a novel and tractable approximation for the signal-to-noise ratio (SNR) distribution after receiver combining. Using this approximation, we derive a simple closed-form expression for the outage probability (OP) composed solely of elementary functions, along with its high-SNR approximation. Furthermore, we analyze the ergodic capacity (EC) of the system and derive a closed-form expression for the EC. The high-SNR approximation of the EC is also presented, revealing the power offset in the high-SNR regime. Monte Carlo simulations validate the high accuracy of the proposed analytical models, demonstrating their effectiveness in capturing the performance of the P2P FAS.

**Index Terms**—Diversity order, ergodic capacity, fluid antenna systems, and outage probability.

## I. INTRODUCTION

The fluid antenna system (FAS) has emerged as a promising technology for next-generation wireless communication systems due to its ability to dynamically adapt its antenna position within a small physical space [1]–[3]. Compared to conventional antenna systems, FAS leverages the fluid nature of conductive materials to achieve superior spatial diversity and improved communication reliability. By allowing the antenna to switch positions among multiple preset ports, FAS can effectively exploit channel variations, reduce interference, and enhance system performance in a flexible and efficient manner. This unique capability positions FAS as a critical enabler for future high-performance communication networks, including 6G and beyond [4].

Despite its advantages, analyzing the delivery performance of FAS remains challenging due to the strong spatial correlation among ports. The ports are typically placed in close proximity within a limited physical space, leading to highly correlated fading channels. As a result, the exact distribution of the FAS channel gain after receiver combining becomes mathematically intractable [5]. Current approximations for the combined SNR distribution in FAS are often highly complex, involving either products of integral forms [6] or summations of special functions [7], which hinder their practical applicability due to

computational inefficiency. Furthermore, while several studies (e.g., [6]–[8]) have attempted to characterize the diversity order of the FAS, the results are typically approximate and lack rigorous mathematical proofs. For instance, the authors of [8] recently proposed a simple approximation for the outage probability (OP) using the asymptotic matching method [9] and derived the diversity order based on this approximation. However, this approach cannot yield the exact diversity order, leaving a gap in understanding the precise diversity order achievable in the FAS.

Motivated by the above challenges, this letter investigates the delivery performance of a point-to-point (P2P) FAS, where the receiver is equipped with a one-dimensional  $N$ -port fluid antenna. The main contributions of this work are summarized as follows.

- For the first time, we provide rigorous mathematical proof to reveal the exact diversity order of the P2P FAS.
- We propose a novel and tractable approximation for the combined SNR distribution, and derive a simple closed-form expression for the OP composed solely of elementary functions, as well as derive the high-SNR approximation.
- We also analyze the ergodic capacity (EC) of the FAS and derive a simple closed-form expression. We further present the high-SNR approximation of the EC, which reveals the power offset in the asymptotic regime.

We validate the high accuracy of the proposed analytical models through extensive Monte Carlo simulations, demonstrating their effectiveness in capturing the performance of the P2P FAS. This work provides novel insights into the fundamental performance limits of the FAS and presents simple, yet accurate, analytical tools for evaluating and optimizing FAS-based wireless communications.

*Notations.* We use  $\mathbb{C}$  to denote the set of complex numbers, and  $|\cdot|$  to represent the magnitude of a complex number.  $\mathbb{E}\{\cdot\}$  and  $\mathbb{P}(\cdot)$  denote the expectation operator and probability, respectively. For a matrix  $\mathbf{A}$ ,  $\mathbf{A}^T$  and  $\mathbf{A}^H$  represent its non-conjugate transpose and conjugate transpose, respectively.

## II. SYSTEM MODEL

We consider a P2P communication system, where a single-antenna transmitter sends signals to a receiver equipped with an  $N$ -port fluid antenna. These  $N$  ports are connected to a single radio-frequency (RF) chain and are evenly placed along a linear dimension of length  $W\lambda$ , where  $\lambda$  is the carrier wavelength. Therefore, the receiver can only select the signal from a single port for decoding. To get the optimal combined SNR, the receiver dynamically selects the port that maximizes the instantaneous SNR for each transmission. The SNR at the

EURECOM’s research is partially supported by its industrial members: ORANGE, BMW, SAP, iABG, Norton LifeLock, by the French projects EEMW4FIX (ANR) and PERSEUS (PEPR-5G), by the EU H2030 project CONVERGE, and by a Huawei France funded Chair towards Future Wireless Networks (*Corresponding author: Hui Zhao*).

Hui Zhao and Dirk Slock are with the Communication Systems Department, EURECOM, 06410 Sophia Antipolis, France (email: hui.zhao@eurecom.fr; dirk.slock@eurecom.fr).

Digital Object Identifier 10.1109/LWC.2025.3550820

$n$ -th ( $n = 1, 2, \dots, N$ ) port is given by  $\gamma_n = \bar{\gamma}|h_n|^2$ , where  $\bar{\gamma}$  denotes the average SNR normalized to pathloss and noise power, and  $h_n$  represents the fading channel gain. As a result, the combined SNR takes the form

$$\gamma_{\max} = \max\{\gamma_1, \gamma_2, \dots, \gamma_N\}. \quad (1)$$

### A. Channel Model

Due to the compact physical placement of the antenna ports, the channel gains  $\{h_n\}_{n=1}^N$  are spatially correlated, making the SNR distribution analytically challenging [6], [7]. The spatial correlation among the ports is captured by the correlation matrix  $\mathbf{J} \in \mathbb{C}^{N \times N}$ , which is symmetric and positive semi-definite. As a result, the eigenvalues of  $\mathbf{J}$  are *real and non-negative*. To analyze  $\mathbf{J}$ , we perform eigenvalue decomposition, expressed as  $\mathbf{J} = \mathbf{U}\mathbf{\Lambda}\mathbf{U}^T$ , where  $\mathbf{U}$  is a unitary matrix whose  $n$ -th column corresponds to the eigenvector of  $\mathbf{J}$  associated with the eigenvalue  $\lambda_n$ , the  $n$ -th diagonal element of the diagonal matrix  $\mathbf{\Lambda}$ . Without loss of generality, we assume that the eigenvalues are ordered as  $\lambda_1 \geq \lambda_2 \geq \dots \geq \lambda_N$ . We can write the channel gain  $h_n$  as (cf. [6], [7])

$$h_n = \sum_{m=1}^N u_{n,m} \sqrt{\lambda_m} z_m \quad (2)$$

where  $u_{n,m}$  denotes the  $(n, m)$ -th element of  $\mathbf{U}$ , and  $\{z_m\}_{m=1}^N$  are independently and identically distributed (i.i.d.) complex Gaussian random variables with zero-mean and unit-variance. As  $h_n$  is the summation of multiple Gaussian distributed random variables,  $h_n$  is Gaussian distributed. We can write the channel vector  $\mathbf{h} = [h_1, h_2, \dots, h_N]^T \in \mathbb{C}^{N \times 1}$  as

$$\mathbf{h} = \mathbf{U}\mathbf{\Lambda}^{\frac{1}{2}} \mathbf{z}, \quad (3)$$

where  $\mathbf{z} \triangleq [z_1, z_2, \dots, z_N]^T \in \mathbb{C}^{N \times 1}$ . It is easy to check that the covariance matrix of  $\mathbf{h}$  takes the form

$$\begin{aligned} \mathbb{E}\{\mathbf{h}\mathbf{h}^H\} &= \mathbb{E}\{\mathbf{U}\mathbf{\Lambda}^{\frac{1}{2}} \mathbf{z}\mathbf{z}^H \mathbf{\Lambda}^{\frac{1}{2}} \mathbf{U}^T\} \\ &= \mathbf{U}\mathbf{\Lambda}^{\frac{1}{2}} \mathbb{E}\{\mathbf{z}\mathbf{z}^H\} \mathbf{\Lambda}^{\frac{1}{2}} \mathbf{U}^T = \mathbf{U}\mathbf{\Lambda}\mathbf{U}^T = \mathbf{J}. \end{aligned} \quad (4)$$

### B. Performance Metrics

The OP quantifies the probability that the combined SNR,  $\gamma_{\max}$ , falls below a predefined threshold  $\gamma_{\text{th}}$ , representing the minimum required SNR for reliable communication. Mathematically, it is expressed as

$$\text{OP} = \mathbb{P}(\gamma_{\max} < \gamma_{\text{th}}). \quad (5)$$

To better understand the behavior of OP in the high SNR regime, we introduce the concept of diversity order, defined as

$$G = \lim_{\bar{\gamma} \rightarrow \infty} \frac{\ln \text{OP}}{\ln \bar{\gamma}}, \quad (6)$$

The diversity order reflects the rate at which the OP decreases as the average SNR increases. It is a fundamental measure of a system's ability to exploit spatial diversity in fading environments [7]. A higher diversity order indicates that the system can achieve a faster reduction in the OP with increasing SNR, thereby offering greater reliability.

The EC, on the other hand, represents the average achievable rate of the system, defined as

$$\bar{C} = \mathbb{E}\{\ln(1 + \gamma_{\max})\} \text{ nats/s/Hz}. \quad (7)$$

This metric provides insights into the long-term throughput of the system, averaged over all possible channel realizations.

## III. PERFORMANCE ANALYSIS

In this section, we will first analyze the diversity order in Theorem 1, followed by an approximation for the OP presented in Lemma 1. Subsequently, an approximation for the EC is derived in Lemma 2. Additionally, we also provide high-SNR asymptotic results for both the OP and the EC.

### A. Diversity Order of P2P FAS

**Theorem 1.** *The diversity order of the considered P2P FAS equals to the rank of  $\mathbf{J}$ , i.e.,  $G = M \triangleq \text{Rank}\{\mathbf{J}\}$ .*

*Proof.* Let  $|h_{\text{FAS}}|^2 \triangleq \max\{|h_1|^2, \dots, |h_N|^2\}$  denote the combined channel gain of the considered P2P FAS. To derive the diversity order, we first note that

$$\frac{1}{N} \sum_{n=1}^N |h_n|^2 = \frac{1}{N} \|\mathbf{h}\|^2 \leq |h_{\text{FAS}}|^2 \leq \|\mathbf{h}\|^2, \quad (8)$$

where  $\|\mathbf{h}\|$  denotes the norm-2 of  $\mathbf{h}$ . For  $\|\mathbf{h}\|^2$ , considering (3), we have that

$$\|\mathbf{h}\|^2 = \mathbf{z}^H \mathbf{\Lambda}^{\frac{1}{2}} \mathbf{U}^T \mathbf{U} \mathbf{\Lambda}^{\frac{1}{2}} \mathbf{z} = \mathbf{z}^H \mathbf{\Lambda} \mathbf{z} = \sum_{n=1}^M \lambda_n |z_n|^2, \quad (9)$$

where  $M$  is the number of non-zero eigenvalues of  $\mathbf{\Lambda}$  (or equivalently, the rank of  $\mathbf{J}$ ). Therefore, we can establish both lower and upper bounds for  $\|\mathbf{h}\|^2$  as follows

$$\lambda_{\min} \sum_{n=1}^M |z_n|^2 \leq \|\mathbf{h}\|^2 = \sum_{n=1}^M \lambda_n |z_n|^2 \leq \lambda_{\max} \sum_{n=1}^M |z_n|^2, \quad (10)$$

where  $\lambda_{\min}$  and  $\lambda_{\max}$  are respectively the minimum and maximum *non-zero* eigenvalues of  $\mathbf{J}$ . Let  $Z = \sum_{n=1}^M |z_n|^2$ , i.e.,  $Z$  is the summation of  $M$  i.i.d. random variables (each exponentially distributed with unit-mean). Then, we have that

$$\frac{\lambda_{\min}}{N} Z \leq \frac{1}{N} \|\mathbf{h}\|^2 \leq |h_{\text{FAS}}|^2 \leq \|\mathbf{h}\|^2 \leq \lambda_{\max} Z. \quad (11)$$

Based on (11), we derive both the upper and lower bounds for the OP, given by

$$\mathbb{P}\left(\lambda_{\max} Z \leq \frac{\gamma_{\text{th}}}{\bar{\gamma}}\right) \leq \text{OP} \leq \mathbb{P}\left(\frac{\lambda_{\min}}{N} Z \leq \frac{\gamma_{\text{th}}}{\bar{\gamma}}\right). \quad (12)$$

Further, we have that

$$\mathbb{P}\left(Z \leq \frac{\gamma_{\text{th}}}{\bar{\gamma} \lambda_{\max}}\right) \leq \text{OP} \leq \mathbb{P}\left(Z \leq \frac{\gamma_{\text{th}} N}{\bar{\gamma} \lambda_{\min}}\right). \quad (13)$$

It is easy to prove that  $Z$  is Gamma distributed with the shape parameter  $M$  and the unit scale parameter. Therefore, the CDF of  $Z$  is of the form

$$F_Z(z) = \mathbb{P}(Z \leq z) = \frac{1}{\Gamma(M)} \Upsilon(M, z). \quad (14)$$

where  $\Gamma(\cdot)$  and  $\Upsilon(\cdot, \cdot)$  are the Gamma function and the lower incomplete Gamma function [10] respectively. As  $z \rightarrow 0$ , the CDF of  $Z$  can be simplified as

$$F_Z(z) = \frac{1}{\Gamma(M)} \Upsilon(M, z) = \frac{z^M}{M\Gamma(M)} + o(z^M). \quad (15)$$

Therefore, as  $\bar{\gamma} \rightarrow \infty$  (high SNR), by omitting the higher order terms in (15), we can simplify (13) as

$$\frac{1}{M\Gamma(M)} \left( \frac{\gamma_{\text{th}}}{\bar{\gamma}\lambda_{\text{max}}} \right)^M \leq \text{OP} \leq \frac{1}{M\Gamma(M)} \left( \frac{\gamma_{\text{th}}N}{\bar{\gamma}\lambda_{\text{min}}} \right)^M. \quad (16)$$

For the lower and upper bounds in the above, we have the limits respectively

$$\lim_{\bar{\gamma} \rightarrow \infty} -\frac{1}{\ln \bar{\gamma}} \ln \left( \frac{1}{M\Gamma(M)} \left( \frac{\gamma_{\text{th}}}{\bar{\gamma}\lambda_{\text{max}}} \right)^M \right) = M, \quad (17)$$

$$\lim_{\bar{\gamma} \rightarrow \infty} -\frac{1}{\ln \bar{\gamma}} \ln \left( \frac{1}{M\Gamma(M)} \left( \frac{\gamma_{\text{th}}N}{\bar{\gamma}\lambda_{\text{min}}} \right)^M \right) = M. \quad (18)$$

Considering (16)–(18) and the Squeeze Theorem [11, Thm. 3.3.6], we finally have that

$$G = \lim_{\bar{\gamma} \rightarrow \infty} -\frac{\ln \text{OP}}{\ln \bar{\gamma}} = M, \quad (19)$$

which concludes the proof. ■

**Remark 1.** This work presents, for the first time, a rigorous mathematical proof of the diversity order in P2P FAS and reveals its exact value. In contrast, prior works such as [7, Thm. 3] and [8, Prop. 2] derive the diversity order based on various approximations. Specifically, [7, Thm. 3] provides a numerical approximation for the diversity order, while [8, Prop. 2] estimates the diversity order as  $N$  using the asymptotic matching method. However, since these results rely on approximations, they do not reveal the exact diversity order, as clearly identified in Theorem 1.

### B. Outage Probability and Ergodic Capacity

Inspired by the fact that  $\|\mathbf{h}\|^2 = \sum_{n=1}^M \lambda_n |z_n|^2$  and the analysis that the diversity order is  $M$ , which indicates the FAS's ability to combine signals from  $M$  paths over independent Rayleigh fading channels, we approximate  $|h_{\text{FAS}}|^2$  as

$$\begin{aligned} |h_{\text{FAS}}|^2 &= \max\{|h_1|^2, \dots, |h_N|^2\} \\ &\approx Z_{\text{max}} \triangleq \max\{\lambda_1 |z_1|^2, \dots, \lambda_M |z_M|^2\}. \end{aligned} \quad (20)$$

Considering the approximation in (20), we have the results for the OP in Lemma 1.

**Lemma 1.** For a given SNR threshold  $\gamma_{\text{th}}$ , the OP of the considered P2P FAS can be approximated as follows

$$\text{OP} \approx \prod_{n=1}^M \left( 1 - \exp\left(-\frac{\gamma_{\text{th}}}{\lambda_n \bar{\gamma}}\right) \right). \quad (21)$$

In the high-SNR regime, i.e.,  $\bar{\gamma} \rightarrow \infty$ , we can further approximate the OP as follows

$$\text{OP} \approx \frac{\gamma_{\text{th}}^M}{\prod_{n=1}^M \lambda_n} \bar{\gamma}^{-M}. \quad (22)$$

*Proof.* We can derive the CDF of  $Z_{\text{max}}$  by

$$\begin{aligned} F_{Z_{\text{max}}}(z) &= \Pr \{ \max\{\lambda_1 |z_1|^2, \dots, \lambda_M |z_M|^2\} \leq z \} \\ &= \prod_{n=1}^M \Pr \left\{ |z_n|^2 \leq \frac{z}{\lambda_n} \right\} \stackrel{(a)}{=} \prod_{n=1}^M \left( 1 - \exp\left(-\frac{z}{\lambda_n}\right) \right), \end{aligned} \quad (23)$$

where (a) follows from the fact that  $|z_n|^2$  is exponentially distributed with unit-mean. Based on the approximation in (20), we can approximate the CDF of the combined SNR as

$$F_{\gamma_{\text{max}}}(x) \approx \prod_{n=1}^M \left( 1 - \exp\left(-\frac{x}{\lambda_n \bar{\gamma}}\right) \right) \quad (24)$$

which leads to (21) by substituting  $x$  with  $\gamma_{\text{th}}$ .

In high SNR, i.e.,  $\bar{\gamma} \rightarrow \infty$ , by truncating the Taylor series of the exponential function in the approximate OP up to the first order, i.e.,  $\exp(-x) = 1 - x + o(x)$ , we can derive (22). ■

**Remark 2.** It is worth noting that when the spatial correlation matrix  $\mathbf{J}$  is full rank, the high-SNR asymptotic OP expression in (22) coincides with the corresponding result presented in [7, Thm. 2], although they adopted completely different analytical approaches.

Before presenting the main results for the EC, for a given  $k \in \{1, 2, \dots, M\}$ , we use the notation  $\sum_{\mathbf{n}_k} \triangleq \sum_{1 \leq n_1 < n_2 < \dots < n_k \leq M}$  to denote the summation in the Euler function (cf. [12, Eq. (10.7)]).

**Lemma 2.** The EC in the considered P2P FAS can be approximated as

$$\bar{C} \approx \sum_{k=1}^M (-1)^k \sum_{\mathbf{n}_k} \exp\left(\sum_{j=1}^k \frac{1}{\lambda_{n_j} \bar{\gamma}}\right) \text{Ei}\left(-\sum_{j=1}^k \frac{1}{\lambda_{n_j} \bar{\gamma}}\right) \quad (25)$$

where  $\text{Ei}(\cdot)$  denotes the exponential integral function [10]. In high SNR ( $\bar{\gamma} \rightarrow \infty$ ), we can further simplify the EC as

$$\bar{C} \approx \ln(\bar{\gamma}) - \xi + \sum_{k=1}^M (-1)^k \sum_{\mathbf{n}_k} \ln \left( \sum_{j=1}^k \frac{1}{\lambda_{n_j}} \right) \quad (26)$$

where  $\xi = 0.577 \dots$  is the Euler's constant [10, Eq. (8.367.1)].

*Proof.* The proof is relegated into Appendix I. ■

**Remark 3.** It is important to note that the approximations for OP and EC are also applicable to the two-dimensional fluid antenna, as our analysis relies solely on the eigenvalues of the correlation matrix  $\mathbf{J}$ , which are inherent system properties determined by the specific structure of the FAS.

## IV. NUMERICAL RESULTS

In this section, we compare the performance metrics, including the OP and EC, with Monte Carlo simulation results to validate the accuracy and practicality of the proposed analytical models. To model the spatial correlation matrix  $\mathbf{J}$ , we employ the widely used Jake's model [13], which effectively captures the physical correlation among antenna ports in a one-dimensional fluid antenna, where the ports are closely spaced

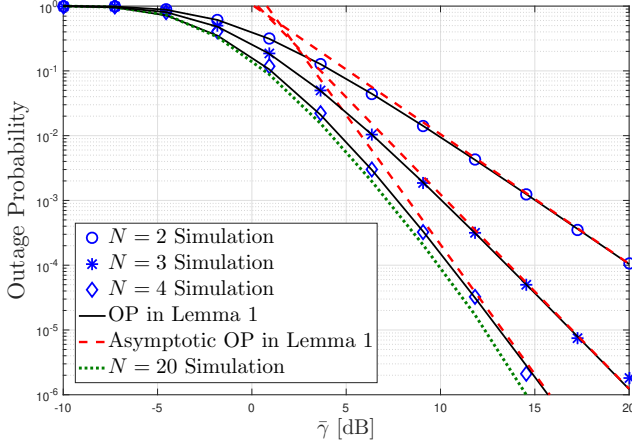


Fig. 1: OP versus  $\bar{\gamma}$  for  $W = 1$  and  $\gamma_{\text{th}} = 1$ .

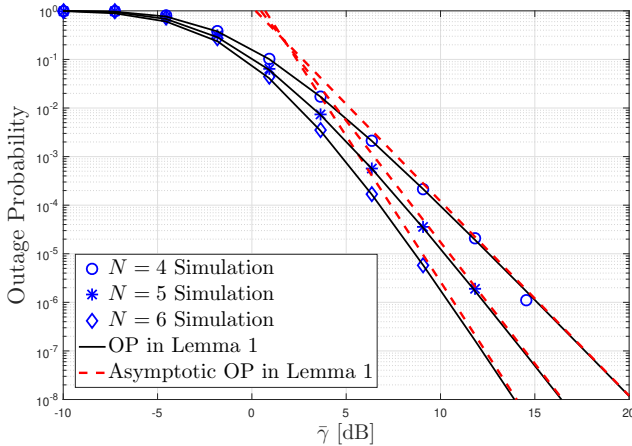


Fig. 2: OP versus  $\bar{\gamma}$  for  $W = 3$  and  $\gamma_{\text{th}} = 1$ .

relative to the carrier wavelength [6], [7]. In this model, the  $(m, n)$ -th entry of  $\mathbf{J}$  is given by

$$J_{m,n} = J_0 \left( 2\pi \frac{(m-n)}{N-1} W \right), \quad (27)$$

where  $J_0(\cdot)$  denotes the zero-order Bessel function of the first kind [10], and  $W$  is the fluid antenna length normalized to the carrier wavelength  $\lambda$ . Based on the spatial correlation model in (27), we generate  $10^7$  channel realizations to compute the sample mean for each Monte Carlo simulation result.

In Fig. 1, we plot the OP versus the average SNR  $\bar{\gamma}$  for  $W = 1$  with different numbers of ports  $N$ . As expected, the OP decreases as  $N$  increases, with a steeper slope reflecting a higher diversity order. However, as  $N$  grows beyond 4 to a large value (e.g.,  $N = 20$ ), the improvement in OP becomes marginal. This behavior aligns with the observations in [7, Table II], where the reference level  $N^*$  is determined numerically to identify the point beyond which increasing  $N$  provides negligible improvement. Theorem 1 provides a theoretical explanation for the existence of  $N^*$ , revealing that the diversity order is fundamentally limited by the rank of the spatial correlation matrix  $\mathbf{J}$ . Specifically, for a fixed physical length  $W$ , increasing  $N$  strengthens the spatial correlation

among closely spaced ports, which restricts the rank of  $\mathbf{J}$  and thus limits the achievable diversity order.

To explore the effect of increasing  $W$ , we plot the OP for  $W = 3$  in Fig. 2. Compared to Fig. 1, the larger physical space allows more ports to be placed with reduced spatial correlation, thereby enhancing the effective diversity order. As  $N$  increases, the OP again improves significantly, and each curve exhibits a steeper slope corresponding to a higher diversity order. In Figs. 1–2, the approximate OP derived in Lemma 1 (solid lines) matches the simulated result (symbols) very well, while the high-SNR asymptotic OP (dashed lines) aligns closely with the simulations in the high-SNR regime, demonstrating the high accuracy of the proposed analytical results in Lemma 1.

Fig. 3 illustrates the EC versus  $\bar{\gamma}$  for  $W = 1$  with different values of  $N$ . As  $\bar{\gamma}$  increases, the EC improves due to the enhanced channel quality. Similar to the OP behavior in Fig. 1, the EC increases with  $N$ , but the improvement becomes marginal for  $N > 4$  due to the limited spatial diversity caused by strong correlations among closely spaced ports. The approximate EC in Lemma 2 (solid lines) closely matches the simulated result (symbols), particularly for  $N = 2$  and  $N = 3$  in Fig. 3. The high-SNR asymptotic EC in Lemma 2 (dashed lines) also demonstrates excellent agreement with the simulations in the high-SNR regime. However, for larger  $N$ , slight mismatches appear. From extensive numerical simulations (omitted due to space limitations), we observe that the slight mismatch arises because the spatial correlation matrix  $\mathbf{J}$  becomes singular or nearly singular when  $N \geq 4$ . Despite slight mismatches when  $N \geq 4$ , numerical results in Fig. 3 indicate that the performance improvement becomes negligible beyond  $N = 4$ . Therefore, in practice, placing more than 4 ports is less meaningful.

We further evaluate the accuracy of the approximate EC in Lemma 2 at the reference level  $N^*$ , where  $\mathbf{J}$  becomes singular or nearly singular, under varying  $N$  and  $W$  in Fig. 4. We consider two specific cases:  $W = 0.5$  and  $W = 4$ . [7, Table II] shows that for  $W = 0.5$ , the reference level is  $N^* = 3$ , and for  $W = 4$ , it increases to  $N^* = 10$ . As shown in Fig. 4, the approximate EC remains highly accurate in both cases. For  $W = 0.5$ , when  $N$  is reduced to 2, the approximate and simulated EC results are nearly indistinguishable, further validating the accuracy of the proposed model. We note that as  $N$  becomes sufficiently large, the reference level  $N^*$  exhibits an asymptotic linear relationship with  $W$  (e.g.,  $2W$ ), as detailed in [14, Coro. 1].

#### A. Validation Under the Optimistic Constant Correlation Model

Let us consider the exceedingly optimistic constant correlation model in [15] where the channel gain for the  $n$ -th port is of the form<sup>1</sup>

$$h_n = \mu Z_0 + \sqrt{1 - \mu^2} Z_n, \quad (28)$$

where  $Z_0, Z_1, \dots, Z_N$  are i.i.d. random variables, each following a complex Gaussian distribution with zero-mean and

<sup>1</sup>The content in Section IV-A was requested by the reviewers of IEEE Wireless Communications Letters but was ultimately omitted from the published version due to space constraints.

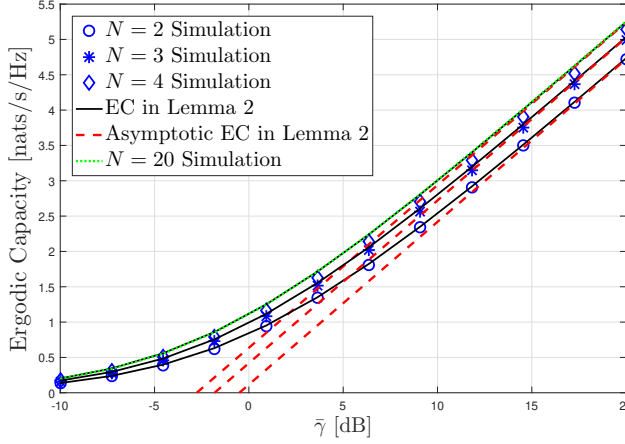


Fig. 3: EC versus  $\bar{\gamma}$  for  $W = 1$ .

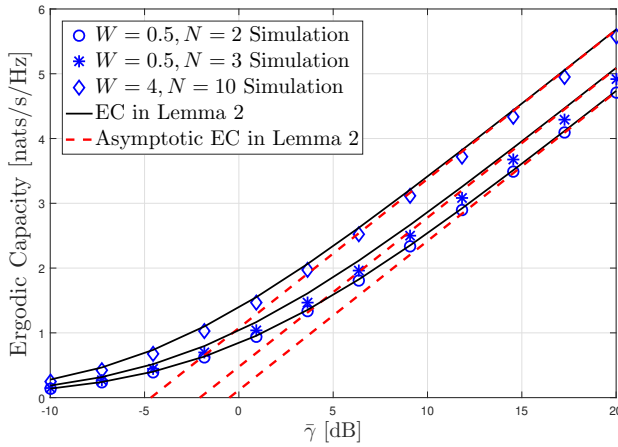


Fig. 4: EC versus  $\bar{\gamma}$  with varying  $N$  and  $W$ .

unit-variance, and  $\mu \in [0, 1]$  specifies the correlation structures of the channels over the ports, defined as follows [15, Eq. (4)]

$$\mu^2 \triangleq \left| \frac{2}{N(N-1)} \sum_{k=1}^{N-1} (N-k) J_0\left(\frac{2\pi kW}{N-1}\right) \right|, \quad (29)$$

which implies that the correlation coefficient between any two distinct ports is always  $\mu^2$ . So the correlation matrix  $\mathbf{J} \in \mathbb{C}^{N \times N}$  is of the form

$$\mathbf{J} = \begin{pmatrix} 1 & \mu^2 & \mu^2 & \cdots & \mu^2 \\ \mu^2 & 1 & \mu^2 & \cdots & \mu^2 \\ \mu^2 & \mu^2 & 1 & \cdots & \mu^2 \\ \vdots & \vdots & \vdots & \ddots & \vdots \\ \mu^2 & \mu^2 & \mu^2 & \cdots & 1 \end{pmatrix} \quad (30)$$

which is a special type of Toeplitz matrix. The corresponding eigenvalues can be easily derived, as follows

$$\lambda_n = \begin{cases} 1 + (N-1)\mu^2, & \text{for } n = 1; \\ 1 - \mu^2, & \text{for } n > 1 \end{cases} \quad (31)$$

which shows that the correlation matrix  $\mathbf{J}$  is always *full-rank*, i.e.,  $N = M$ , as long as  $\mu^2 < 1$ . Alternatively, we can express

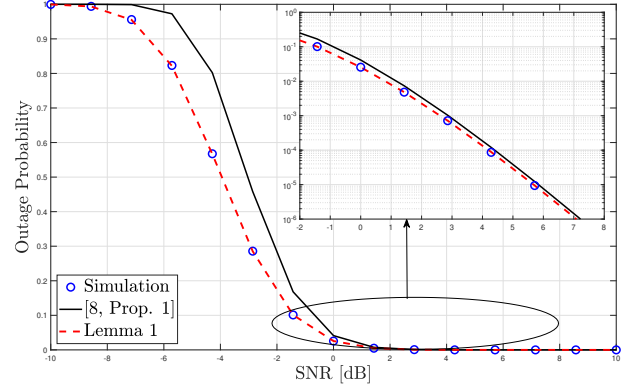


Fig. 5: OP versus  $\bar{\gamma}$  for  $\gamma_{\text{th}} = 1$ ,  $W = 2$  and  $N = 8$  under the optimistic constant correlation model [15]. The red dashed line represents Lemma 1 in the manuscript and the black solid line represents [8, Prop. 1].

the channel vector  $\mathbf{h} = [h_1, h_2, \dots, h_N]^T$  for the  $N$ -port fluid antenna as

$$\mathbf{h} = \mathbf{J}^{\frac{1}{2}} \mathbf{z} \quad (32)$$

where  $\mathbf{z} \in \mathbb{C}^{N \times 1}$  is a random vector whose elements are i.i.d. complex Gaussian distributed random variables with zero-mean and unit-variance.

Under this constant correlation model, and after applying some straightforward mathematical simplifications, the OP approximation in [8, Prop. 1] simplifies to

$$\text{OP} \approx \frac{1}{\Gamma(N)} \Upsilon\left(N, \frac{\gamma_{\text{th}}}{\bar{\gamma}} \left(\frac{\Gamma(N)N}{(1-\mu^2)^{N-1}}\right)^{1/N}\right), \quad (33)$$

where  $\Upsilon(\cdot, \cdot)$  denotes the lower incomplete Gamma function. In contrast, our proposed OP approximation in Lemma 1 under this constant correlation model becomes

$$\begin{aligned} \text{OP} &\approx \prod_{n=1}^N \left(1 - \exp\left(-\frac{\gamma_{\text{th}}}{\bar{\gamma}\lambda_n}\right)\right) \\ &= \left(1 - \exp\left(-\frac{\gamma_{\text{th}}}{\bar{\gamma}(1+(N-1)\mu^2)}\right)\right) \\ &\quad \times \left(1 - \exp\left(-\frac{\gamma_{\text{th}}}{\bar{\gamma}(1-\mu^2)}\right)\right)^{N-1}. \end{aligned} \quad (34)$$

In Fig. 5, it is evident that our proposed method in Lemma 1 achieves significantly higher accuracy than [8, Prop. 1], particularly in the low-SNR regime. However, their difference asymptotically approaches zero as the SNR increases, and both methods exhibit excellent agreement with the exact (simulated) results in the high-SNR regime.

However, as the number of ports  $N$  increases in Fig. 6, [8, Prop. 1] exhibits a noticeable deviation from the simulated results, even in the high-SNR regime. In contrast, our proposed expression in Lemma 1 consistently maintains high accuracy. To further examine scenarios where Lemma 1 may exhibit relatively lower accuracy, we increase  $N$  to 50 in Fig. 7, where a larger OP value leads to a more pronounced discrepancy. Nevertheless, for practical OP values (typically below 0.01 for reliable communications), Lemma 1 continues to provide highly accurate results compared to simulations.

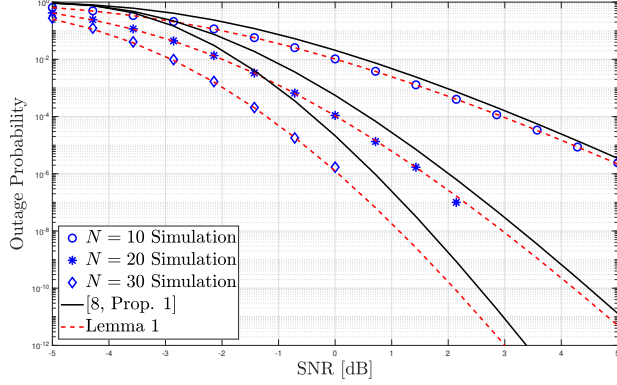


Fig. 6: OP versus  $\bar{\gamma}$  for  $\gamma_{th} = 1$  and  $W = 4$  under the optimistic constant correlation model [15]. The red dashed line represents Lemma 1 in the manuscript and the black solid line represents [8, Prop. 1].

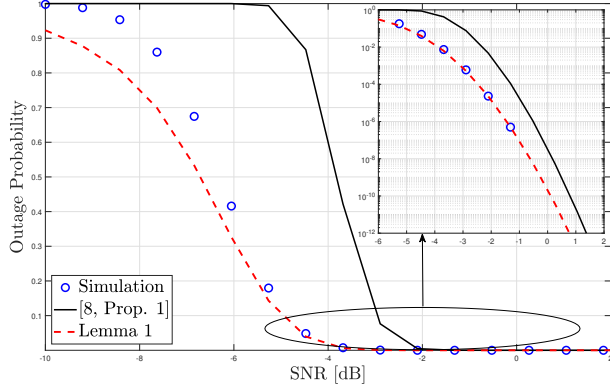


Fig. 7: OP versus  $\bar{\gamma}$  for  $\gamma_{th} = 1$ ,  $W = 4$  and  $N = 50$  under the optimistic constant correlation model [15]. The red dashed line represents Lemma 1 in the manuscript and the black solid line represents [8, Prop. 1].

## V. CONCLUSIONS AND DISCUSSIONS

This letter analyzed the delivery performance of the P2P FAS with a one-dimensional  $N$ -port fluid receiver antenna. We rigorously proved the diversity order of the P2P FAS and proposed a novel approximation for the SNR distribution, enabling a simple closed-form expression for the OP using only elementary functions, from which we also derived the closed-form expression for the EC. Additionally, we presented the high-SNR approximations for both OP and EC, offering key insights into the asymptotic behavior of FAS. The proposed analytical models, validated through Monte Carlo simulations, provide a tractable framework for evaluating FAS performance and lay the foundation for future studies in fluid antenna technology.

For device-to-device (D2D) networks, the applicability of our analytical method depends on the system settings, particularly whether each receiver has global channel state information (CSI). For receivers without global CSI, inter-user interference is usually treated as noise. In this case, the interference effect can be accounted for by reducing the average SNR in our P2P model, providing a practical way to incorporate inter-user interference. On the other hand, if each receiver has global CSI, the interference at different fluid antenna ports is correlated (cf. [16, Eq. (15)]), which aligns with the Fluid Antenna Multiple

Access (FAMA) framework. Addressing this case requires a different approach, which will be explored in future work.

## APPENDIX I: PROOF OF LEMMA 2

By using some integral transforms, we can write the integral for the EC defined in (7) as (cf. [17, Eq. (48)])

$$\bar{C} = \int_0^\infty \frac{1 - F_{\gamma_{\max}}(x)}{1+x} dx. \quad (35)$$

Thanks to the simple OP (i.e., the combined SNR) distribution in (21), we can approximate the EC as

$$\bar{C} \approx \int_0^\infty \frac{1}{1+x} \left[ 1 - \prod_{n=1}^M \left( 1 - \exp\left(-\frac{x}{\lambda_n \bar{\gamma}}\right) \right) \right] dx. \quad (36)$$

Based on the Inclusion-Exclusion Principle [12], we can rewrite the CDF of the combined SNR  $\gamma_{\max}$  as

$$F_{\gamma_{\max}}(x) = 1 + \sum_{k=1}^M (-1)^k \sum_{\mathbf{n}_k} \exp\left(-\sum_{j=1}^k \frac{x}{\lambda_{n_j} \bar{\gamma}}\right). \quad (37)$$

Therefore, we can rewrite (36) as

$$\bar{C} \approx \sum_{k=1}^M (-1)^{k+1} \sum_{\mathbf{n}_k} \int_0^\infty \frac{\exp\left(-\sum_{j=1}^k \frac{x}{\lambda_{n_j} \bar{\gamma}}\right)}{1+x} dx. \quad (38)$$

With the help of [10, Eq. (3.353.5)], we can solve (38) in the closed-form expression, as shown in (25).

To derive the asymptotic EC in high SNR, following the asymptotic method in [18], we first approximate the exponential integral function  $\text{Ei}(-x)$  by

$$\text{Ei}(-x) \rightarrow \ln(x) + \xi, \text{ as } x \rightarrow 0. \quad (39)$$

Then, as  $\bar{\gamma} \rightarrow \infty$ , we can approximate the EC in (25) as

$$\begin{aligned} \bar{C} &\approx \sum_{k=1}^M (-1)^k \sum_{\mathbf{n}_k} \left( \ln\left(\sum_{j=1}^k \frac{1}{\lambda_{n_j} \bar{\gamma}}\right) + \xi \right) \\ &= \left( -1 + 1 + \sum_{k=1}^M (-1)^k \sum_{\mathbf{n}_k} \left( -\ln(\bar{\gamma}) + \xi \right) \right) \\ &\quad + \sum_{k=1}^M (-1)^k \sum_{\mathbf{n}_k} \ln\left(\sum_{j=1}^k \frac{1}{\lambda_{n_j}}\right) \\ &\stackrel{(a)}{=} \left( -1 + \prod_{n=1}^M (1-1) \right) \left( -\ln(\bar{\gamma}) + \xi \right) \\ &\quad + \sum_{k=1}^M (-1)^k \sum_{\mathbf{n}_k} \ln\left(\sum_{j=1}^k \frac{1}{\lambda_{n_j}}\right), \quad (40) \end{aligned}$$

where (a) follows from the inverse of the Inclusion-Exclusion Principle, and which finally yields the asymptotic EC in (26).

## REFERENCES

- [1] K. Wong, A. Shojaeifard, K. Tong, and Y. Zhang, "Fluid antenna systems," *IEEE Trans. Wireless Commun.*, vol. 20, no. 3, pp. 1950–1962, Mar. 2021.
- [2] K.-K. Wong, K.-F. Tong, Y. Shen, Y. Chen, and Y. Zhang, "Bruce lee-inspired fluid antenna system: Six research topics and the potentials for 6G," *Frontiers Commun. Netw.*, vol. 3, p. 853416, Mar. 2022.
- [3] W. Ma, L. Zhu, and R. Zhang, "MIMO capacity characterization for movable antenna systems," *IEEE Trans. Wireless Commun.*, vol. 23, no. 4, pp. 3392–3407, Apr. 2024.
- [4] A. Shojaeifard *et al.*, "MIMO evolution beyond 5G through reconfigurable intelligent surfaces and fluid antenna systems," *Proc. IEEE*, vol. 110, no. 9, pp. 1244–1265, Sep. 2022.
- [5] K. N. Le, "A review of selection combining receivers over correlated Rician fading," *Digit. Signal Process.*, vol. 88, pp. 1–22, May 2019.
- [6] M. Khammassi, A. Kammoun, and M.-S. Alouini, "A new analytical approximation of the fluid antenna system channel," *IEEE Trans. Wireless Commun.*, vol. 22, no. 12, pp. 8843–8858, Dec. 2023.
- [7] W. K. New, K.-K. Wong, H. Xu, K.-F. Tong and C.-B. Chae, "Fluid antenna system: New insights on outage probability and diversity gain," *IEEE Trans. Wireless Commun.*, vol. 23, no. 1, pp. 128–140, Jan. 2024.
- [8] J. D. Vega-Sánchez, A. E. López-Ramírez, L. Urquiza-Aguiar, and D. P. M. Osorio, "Novel expressions for the outage probability and diversity gains in fluid antenna system," *IEEE Wireless Commun. Lett.*, vol. 13, no. 2, pp. 372–376, Feb. 2024.
- [9] F. R. A. Parente and J. C. S. S. Filho, "Asymptotically exact framework to approximate sums of positive correlated random variables and application to diversity-combining receivers," *IEEE Wireless Commun. Lett.*, vol. 8, no. 4, pp. 1012–1015, Aug. 2019.
- [10] I. S. Gradshteyn and I. M. Ryzhik, *Table of integrals, series, and products*, 7th ed. Academic press, 2007.
- [11] H. H. Sohrab, *Basic Real Analysis*, 2nd ed. Springer, 2014.
- [12] J. H. van Lint and R. M. Wilson, *A Course in Combinatorics*, 2nd ed. Cambridge University Press, 2001.
- [13] G. L. Stüber and G. L. Steuber, *Principles of Mobile Communication*, vol. 2. Cham, Switzerland: Springer, 1996.
- [14] P. Ramírez-Espinosa, D. Morales-Jimenez, and K.-K. Wong, "A new spatial block-correlation model for fluid antenna systems," *IEEE Trans. Wireless Commun.*, vol. 23, no. 11, pp. 15 829–15 843, Nov. 2024.
- [15] K.-K. Wong, K.-F. Tong, Y. Chen, and Y. Zhang, "Closed-form expressions for spatial correlation parameters for performance analysis of fluid antenna systems," *Electron. Lett.*, vol. 58, no. 11, pp. 454–457, 2022.
- [16] K.-K. Wong and K.-F. Tong, "Fluid antenna multiple access," *IEEE Trans. Wireless Commun.*, vol. 21, no. 7, pp. 4801–4815, Jul. 2022.
- [17] H. Zhao, Z. Liu, L. Yang, and M.-S. Alouini, "Secrecy analysis in DF relay over generalized- $K$  fading channels," *IEEE Trans. Commun.*, vol. 67, no. 10, pp. 2653–2661, Oct. 2019.
- [18] H. Zhao, Z. Liu, and M.-S. Alouini, "Different power adaption methods on fluctuating two-ray fading channels," *IEEE Wireless Commun. Lett.*, vol. 8, no. 2, pp. 592–595, Apr. 2019.